International Journal of Materials Chemistry and Physics
Vol. 1, No. 3, 2015, pp. 242-245
http://www.aiscience.org/journal/ijmcp

Structural and Electrical Properties of Li_2O-TiO_2 System in Presence of Water

R. Alvarez Roca[1, *], F. Guerrero Zayas[2]

[1]LIEC, Chemistry Deparment, Federal University of São Carlos, São Carlos-SP, Brazil
[2]Physics Department, ICE, Federal University of Amazonas, Manaus-AM, Brazil

Abstract

The influence of Li_2O and humidity on structural and electrical properties of TiO_2 ceramics are presented for two different concentrations (0.02 and 0.06 mol%). The X-Ray analysis shows a single phase compound for 0.02, due to the Li incorporation into the rutile, while the pattern for the 0.06 composition shows two phases. The structural effects are corroborated by Infrared Spectroscopy where the vibrational modes are discussed for each composition. The electrical behavior is also shown at room temperature and for each composition using a.c. measurement. The effect of Li_2O addition on water adsorption mechanism as well as the humidity sensibility is analyzed. An equivalent circuit, from impedance spectroscopy, is proposed and the physical processes that take place inside the ceramic are described.

Keywords

TiO_2, Humidity, Electrical Properties

Received: August 11, 2015 / Accepted: September 5, 2015 / Published online: Aepetmber 14, 2015

1. Introduction

In recent years, ceramic humidity sensors are widely used for monitoring and controlling in domestic and industrial environments. In comparison with other materials, they present most thermal stability and chemical resistance, superior sensing properties and high mechanical strength [1-6]. In order to improve sensing properties in ceramics the doping is a procedure widely used. It can result in the incorporation of dopant in the crystalline structure and/or in segregation of secondary phase producing ceramic composites [4, 6-15]. The doping effects on the humidity sensitivity can be either by enhancing electrical parameters (changing resistance and capacitance) or/and by optimizing microstructural characteristics (open porosity). Many humidity sensor material have shown a better response sensitivity when Li-doped the material [6, 9, 13-15] in comparison whit other cations (H, Na, Cs).

As a ceramic sensor, TiO_2 is very attractive because of its high efficiency, stability, and low cost [3, 6, 9, 16-18]. Water absorption on TiO_2 rutile is an interesting example of a simple surface chemical process with significant applications.

Recently, we reported the electrical behaviour for xLi-TiO_2 ($0 \leq x \leq 0.02$ in mol %) at middle temperature range [19]. For this concentration range, the rutile is the only system phase. In the present work, the structural and electrical properties of Li_2O-TiO_2 system are examined for two concentrations at room temperature. Lithium and water effects on the rutile is analysed by ac measurements with the Impedance Spectroscopy technique. Employing this technique, the humidity effects in porous system have been widely reported by monitoring the ac conductivity [6, 8, 13, 17, 20, 21]. The role of each part of the material in the electrical conduction process can be determined on the basis of measurements and an equivalent circuit model.

* Corresponding author
E-mail address: cortes116@yahoo.es (R. A. Roca)

2. Experimental Procedure

The samples were prepared by a conventional solid state reaction process. The raw materials used were analytical grade TiO_2 (Merck) and Li_2O (Merck). The molar composition used in TiO_2-x mol% Li_2O are x=0.02, namely TL2, and x=0.06, namely TL6. The ceramics powder was characterizes by X-Ray Diffraction (XRD) analysis (Rigaku Rotaflex RU200B using CuKα radiation) and Fourier Transformed Infrared (FT-IR). Pellets with 10 mm diameter and 1.5 mm thickness were elaborated by pressed under 154 MPa. The green samples were then sintered in air according set in table 1. The relative density (RD, in % of Theory Density) was obtained by Archimedes technique and listed in table 1. Impedance Spectroscopy (IS) measurements were performed at 60 % of relative humidity (r.h.) using a HP4194A impedance analyzer with silver electrodes in the ceramic parallel faces.

3. Results and Discussion

In according with XRD analysis, figure 1, for composition x = 0.02 (TL2) no other phase beside TiO_2 rutile was observed. For TL6, the XRD pattern shows that ceramic sample include TiO_2 rutile and $Li_2Ti_3O_7$ phase. For concentrations until x=0.02, Li incorporation mechanisms via interstitial only, by computational simulation [22], and mixed (interstitial and substitutional), by experimental techniques [19], have been reported.

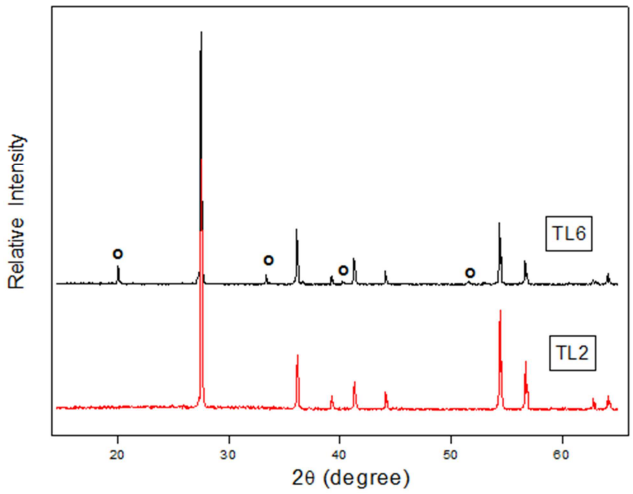

Figure 1. XRD diffraction patterns of powdered Li-doped TiO_2 for 2 and 6 % (circle show more $Li_2Ti_3O_7$ significant peak).

The structural parameters are shown in the table 1. Slight variations in the parameters are observed and, given the experimental error, can us conclude that the Li incorporation doesn't change the cell parameters significantly.

Table 1. Sintering and Structural Characteristics.

Sample	Sintering		Density	Lattice parameter (Å)	
	Temp. (°C)	Time (h.)	(%)	a	c
TiO_2	1200	1	61.9 ‡	4.590 +	2.950 +
TL_2	1100	1	68.1	4.586	2.955
TL_6	1100	1	71.4	4.589	2.958

‡ Reference [8]; + Reference [23]

Li incorporation in rutile for interstitial mechanism has showed a strong preference into octahedral site. Li should then incorporate in TiO_2 according equation (1). Conservation of overall charge neutrality under insertion generates an electron for each Li^+ ion positively charges. This charge compensating electrons can be localized at Ti ions creating Ti^{3+} states.

$$Li_2O + TiO_2 \rightarrow 2Li_i' + O_O^x + 2e\bullet \quad (1)$$

The relative density for both samples is showed in table 1. Bigger relative densities are observed with regard to the pure TiO_2 sintered with approximately similar conditions. This demonstrates that both Li incorporation in the structure and the $Li_2Ti_3O_7$ phase favours the sintering processes. This is contrary to the necessary open porosity for optimal sensing performance.

In the far FT-IR spectrum, see figures 2(a), the multipeak appearing at 2800-3100 cm^{-1} assigned to the stretching vibration of hydroxyl group, which is confirmed by bending modes poorly observed in the expected region. The multipeak is consistent with the bond of acidic H^+ ions with octahedral oxygen observed in oxides with protonic conductivity.

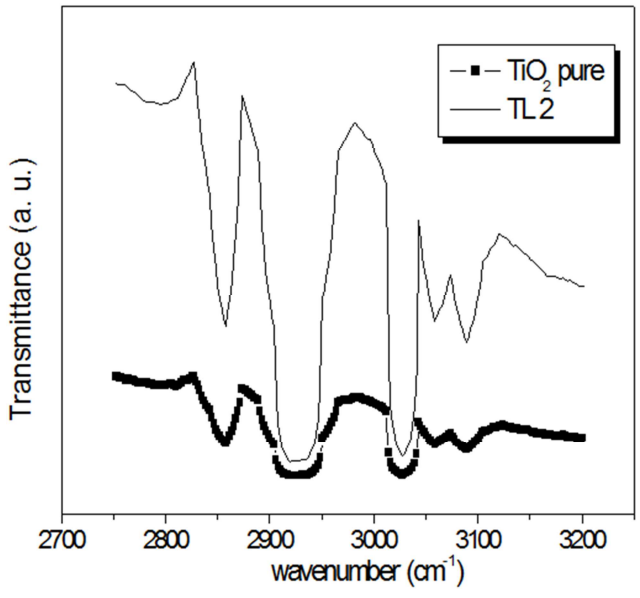

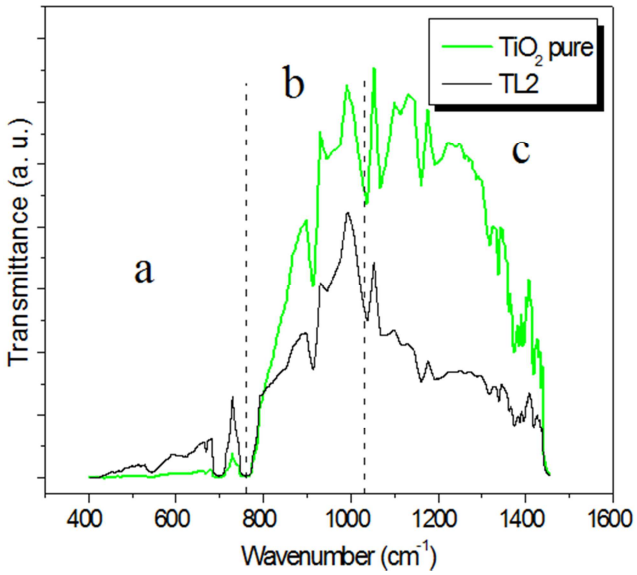

Figure 2. Far (a) and middle (b) FT-IR spectrum of TL2 compared with TiO_2 pure. In (b) tree regions are displayed.

The figure 2(b) shows the middle FT-IR spectrum. The spectrum can be analysed in three regions which reveal the following facts:

i) The modes in region a can be assigned to titanium octahedraly coordinated to oxygen in TiO_6 octahedral in the rutile structure. The very broader modes for TL2 indicated that the Li insertion in the rutile can cause more disorder in the structure.

ii) The bands in region b (800-1050 cm^{-1}) usually can be appear for deformation vibration of metal-OH bonding as well as bending motion of bound H_2O.

iii) The region c (1100-1400 cm^{-1}) may be assigned to the characteristics Ti-O-Ti.

In the ii) and iii) the intensity decreasing of the TL2 peak may be by light absorption by free carrier coming from Ti^{3+}.

Figure 3 shows the IS spectra for TL2 and TL6 samples. These shows only one semicircle ascribed to a grain surface contribution; therefore, the electrical properties are determined more by the grain surface characteristics than by other regions. The sample conductivity is obtained for the intercept of the semicircle with the real axis. As it is observed in the figure 3, the TL2 superficial conductivity is increased with relationship to the TL6.

The Li doping can increase the number of water chemisorption site due to the formation of a higher number of surface defect sites and strong local electrostatic field performing it in good polarise: dissociate sites for water molecule [2]. On the other way, the presence of the $Li_2Ti_3O_7$, which doesn't present the TiO_2 humidity-sensitivity characteristic, reduces the surface composition with high activity of water absorption/dissociation and therefore the charge carried number is reduced increasing thus impedance.

In order to a better understanding of the physics process that take place in the material, we obtained the equivalent circuit (EC), see figure 3. The parameters of each fitting were determined using a non-linear least-square fitting algorithm [24]. The values and the physical meaning of the EC element are presented in the table 2.

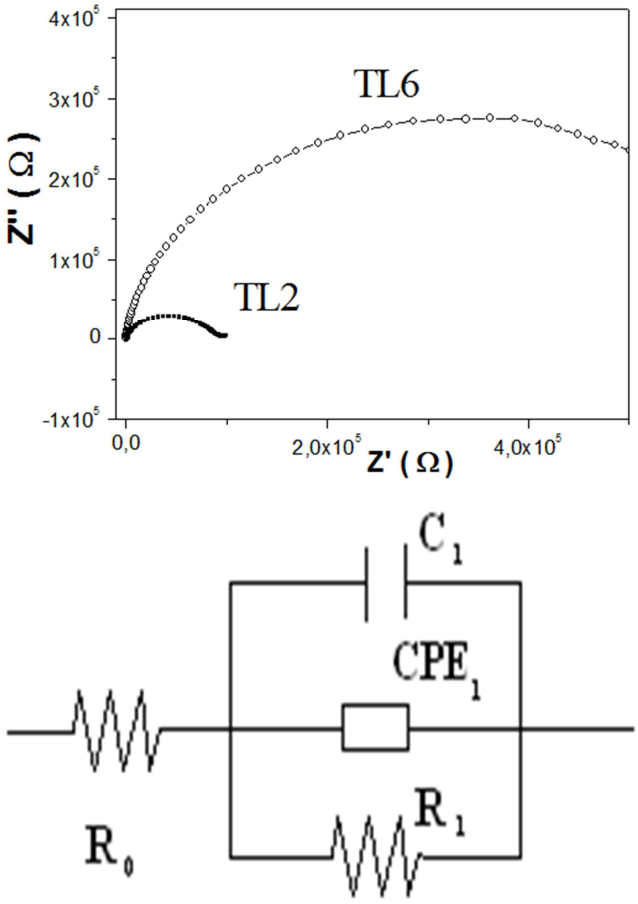

Figure 3. Impedance Spectroscopy for TL2 and TL6 samples at 25 ºC and 60% r.h. and equivalent circuit.

Table 2. Values for each equivalent circuit element.

Physics process	Element	TL2	TL6
Intragrain resistance	R_o (Ω)	40	180
Surface grain capacity	C_1 (F)	$6{,}17\cdot10^{-11}$	$0{,}85\cdot10^{-11}$
Physically adsorbed water	Q_1(F s^{n-1})	$6{,}61\cdot10^{-9}$	$1{,}33\cdot10^{-9}$
	n_1	0.67	0.63
Intergrain surface resistance	R_1 (Ω)	$9{,}08\cdot10^{4}$	$7{,}19\cdot10^{5}$

The Li ions intercalated inside the structure will provide more mobile charge and thus contribute to electrical conduction increasing R_o. The Li addition also increases the number of water adsorption sites in the surface and, correspondingly, the interfacial polarization which is reflecting in the value of the superficial capacity C_1 listed for TL2. The relaxation times, τ=RC, for the semicircles in both samples is approximately the same. This can suggest the same interfacial polarization mechanism. The higher water

adsorption and their surface protonic conduction, originating from hydronium, enhances the surface conduction, displayed in decreasing of R_1 for TL2.

To interpret the conduction, polarization and diffusion processes that occur in a ceramic material in the presence of water molecules, the IS and a.c. measurements were usually used [7, 8, 17, 18, 21]. But in several of these works an EC not is proposed. In contrast, in our work the explanation and comprehension of the EC and their circuit elements values is showed. The relation between the EC elements and the physical behavior observed for specific conditions in the present study allow a better interpretation and understanding of the different processes involved.

4. Conclusions

The structural and electrical characteristics of Li_2O-TiO_2 system in presence of water at room temperature were studied. The obtained experimental results confirm that doping is a way of changing material behavior. The Li incorporation increases the structural disorder as well as generates free charges that produce changes in the vibration bands intensities of the hydrated rutile.

The electrical effects observed can be explained by the doping mechanism and it is depends strongly on the Li incorporation. The equivalent circuit for electrical response is presented which allows to better understanding the diverse charge transport and relaxation mechanisms.

References

[1] Yamazoe, N., Simizu, Y., (1986). Humidity sensors: principles and applications. *Sens. Actuators*, 10: 379–398.

[2] Kulwicki, B.M., (1991). Humidity sensors. *J. Am. Ceram. Soc.*, 74 (4) 697–708.

[3] Traversa, E. (1995). Ceramic sensors for humidity detection: the state of-the-art and future developments. *Sens. Actuators B*, 23: 135–156.

[4] Chen, Z. and Lu, C. (2005). Humidity Sensors: A Review of Materials and Mechanisms. *Sensor Lett.*, 3: 274-295.

[5] Carpenter, M. A., Mathur, S. and Kolmakov, A. (Eds.), (2013). Metal Oxide Nanomaterials for Chemical Sensors, Springer, NY.

[6] Farahani, H., Wagiran, R. and Hamidon, M. N. (2014). Humidity Sensors Principle, Mechanism, and Fabrication Technologies: A Comprehensive Review. *Sensors*, 14: 7881-7939.

[7] Katayama, K., Hasegawa, K., Takahashi, Y., Akiba, T., Yanagida, H. (1990). Humidity Sensitivity of Nb_2O_5-Doped TiO_2 Ceramics. *Sens. Actuators A Phys.*, 24: 55–60.

[8] Yeh, Y. Ch., Tseng, T.Y. and Chang, D. (1990). Electrical Properties of TiO_2-$K_2Ti_6O_{13}$ Porous Ceramic Humidity Sensor. *J. Am. Ceram. Soc*. 73: 1992-1998.

[9] Jain, M.K., Bhatnagar, M.C., Sharma, G.L. (1999). Effect of Li doping on ZrO_2–TiO_2 humidity sensor, *Sens. Actuators B* 55: 180–185.

[10] Ying, J., Wan, C., He, P. (2000). Sol-Gel Processed TiO_2-K_2O-$LiZnVO_4$ Ceramic Thin Films as Innovative Humidity Sensors. *Sens. Actuators B Chem*. 62: 165–170.

[11] Zaleska, A. (2008). Doped-TiO_2: A Review, *Recent Patents Eng.*, 2: 157-164.

[12] Anbia, M., and Fard, S.E.M. (2011). Improving Humidity Sensing Properties of Nanoporous TiO_2-10 mol% SnO_2 Thin Film by Co-Doping with La^{3+} and K^+. *Sens. Actuators B Chem*., 160: 215-221.

[13] Golonka, L.J., Licznerski, B. W., Nitsch, K. and Teterycs H. (1997). Thick-film humidity sensors, *Meas. Sci. Technol*. 8:92-98.

[14] Suresh, A. M. E., Magdalane, C. M. and Nagaraja, K S. (2002). Zinc(II) Oxide–Yttrium(III) Oxide Composite Humidity Sensor *Phys. Stat. Sol. (a)* 191: 230-234.

[15] Geng, W., Wang, R.; Li, X., Zou, Y., Zhang, T., Tu, J., He, Y., and Li, N. (2007). Humidity Sensitive Property of Li-Doped Mesoporous Silica SBA-15. *Sens. Actuators B Chem*., 127: 323–329.

[16] Montesperelli, G., Pumo, A., Traversa, E., Bearzotti, A., Montenero, A., and Gnappi, G. (1995). Sol-Gel Processed TiO_2-Based Thin Films as Innovative Humidity Sensors. *Sens. Actuators B Chem.*, 25: 705–709.

[17] Garcia-Belmonte, G., Kytin, V., Dittrich, T. and Bisquert, J. (2003). Effect of humidity on the ac conductivity of nanoporous TiO_2, *J Appl. Phys*., 94: 5261-5264.

[18] Wang, Z., Shi, L., Wu, F., Yuan, S., Zhao, Y. and Zhang, M. (2011). The sol–gel template synthesis of porous TiO_2 for a high performance humidity sensor, Nanotechnology, 22: 275502.

[19] Alvarez Roca, R., Guerrero, F., Eiras, J. A. and Guerra, J.D.S. (2015). Structural and electrical properties of Li-doped TiO_2 rutile ceramics, *Ceram. Int.*, 41: 6281–6285.

[20] Alvarez Roca, R., Guerrero, F., Garcia-Belmonte, G. and Bisquert, J. (2002). Study of the humidity effect in the electrical response of the $KSbMoO_6$ ionic conductive ceramic at low temperature, *J. Mater. Sci. Eng., B* 90: 291-295.

[21] Faia, P.M., Ferreira, A.J., and Furtado, C.S. (2009). Establishing and Interpreting an Electrical Circuit Representing a TiO_2-WO_3 Series of Humidity Thick Film Sensors. *Sens. Actuators B Chem*., 140: 128–133.

[22] Koudriachova, M. V., Harrison, N. M. and de Leeuw, S. W. (2002) Density-functional simulations of lithium intercalation in rutile. *Phys. Rev.*, *B* 65: 235423.

[23] Burdett, J. K., Hunghbanks, T., Miller, G. J., Richardson, J. W. and Smith, J. V. (1987). Structural-electronic relationships in inorganic solids: powder neutron diffraction studies of the rutile and anatase polymorphs of titanium dioxide at 15 and 295 K, *J. Am. Chem. Soc.*, 109: 3639-3646.

[24] van Hassel, B. A., Boukam, B. A. and Burggraaf, A. J. (1992). Oxygen transfer properties of ion-implanted yttria-stabilized zirconia *Solid. State Ionic* 53-56: 890-903.